Annals of Biomedical Engineering, Vol. 34, No. 8, August 2006 *(© 2006)* pp. 1247–1258
DOI: 10.1007/s10439-006-9134-4

Evolution of Oxygen and Glucose Concentration Profiles in a Tissue-Mimetic Culture System of Embryonic Stem Cells

DAVID M. COCHRAN,[1] DAI FUKUMURA,[1] MAREK ANCUKIEWICZ,[1] PETER CARMELIET,[2] and RAKESH K. JAIN[1]

[1]Department of Radiation Oncology, Massachusetts General Hospital,100 Blossom Street, Cox-7, Boston, Massachusetts 02114 and [2]Center for Transgene Technology and Gene Therapy, Flanders Interuniversity Institute for Biotechnology (VIB), University of Leuven, Campus Gasthuisberg, Herestraat 49, B-3000, Leuven, Belgium

(Received 1 September 2005; accepted 9 May 2006; published online: 11 July 2006)

Abstract—A tissue-mimetic culture system (TMCS) in which cells are sandwiched between two glass slides provides an ideal microenvironment for studying the effects of oxygen and nutrient gradients on cells in culture. A mathematical model was utilized to predict the time course of the development of oxygen and glucose concentration gradients within the TMCS. Oxygen and glucose consumption rates of mouse embryonic stem cells were measured as parameters for the model. The model predicts oxygen and glucose concentration profiles directly using a single experimentally controlled variable, the seeding density of cells within the system. The model predicts that the time required for the gradients to reach steady state is inversely related to the cell density, and the penetration depth of the gradients into the TMCS is inversely related to the square root of the cell density. Experimental oxygen concentration measurements were performed at a cell density of 9.1×10^6 cells cm^{-3}, and the gradient was found to develop to a steady-state profile within 20 min and penetrate approximately 2 mm into the TMCS, consistent with the theoretical predictions. This model and the TMCS provide useful tools for investigating the effect of the metabolic microenvironment on cells in culture.

Keywords—Mathematical modeling, Cancer, Hypoxia, Stem cell biology, Tissue-mimetic culture.

ABBREVIATIONS

TMCS	tissue-mimetic culture system
ES cell	embryonic stem cell
HIF	hypoxia-inducible factor
OBS	Oxygen biosensor
OCR	oxygen consumption rate

INTRODUCTION

Stem cell therapy is a promising field of research for the development of regenerative medicine technologies. Often, the external conditions that stem cells experience are modulated to control the fate of differentiation of stem cells. However, the effects of local changes and gradients in the microenvironment on stem cells are often ignored. Here we develop a system to allow the predictable control of the oxygen and glucose levels experienced locally in an assay that will allow the assessment of stem cell biology under different conditions. In addition, the system developed has broader applications in the area of tumor biology and the study of microenvironmental effects on the response of cells to pharmaceuticals.

To achieve this aim, a tissue-mimetic culture system (TMCS) was used in which cells are grown between two glass slides separated by a fixed distance. This system was initially described as an *in vitro* tumor analog, analogous to multicellular spheroids in mimicking the gradients of oxygen, nutrients, and waste products that develop within a growing tumor.[17] The advantages to using the TMCS over the spheroid system are that cells under the entire gradient can be monitored microscopically without fixation and sectioning[15,17] and that the viable region of the TMCS has been shown to be an order of magnitude larger than the viable rim of a spheroid, which is often only a few cell layers thick.[17] The disadvantage of the TMCS is that like any monolayer *in vitro* system, there is no three-dimensional cell-cell contact. However, for the purposes of investigating the effects of the metabolic microenvironment on cells in culture, the TMCS provides the desirable features of 1) stable and controllable oxygen and nutrient gradients, 2) a region of interest large enough to monitor the cell migration, cell-cell interactions, apoptosis, proliferation, or any other microscopically observable behavior of numerous cells simultaneously, and 3) the ability to monitor the system microscopically in real time, allowing for assessment of the kinetics of these behaviors. The gradients within the TMCS are somewhat "tunable," in that the steepness of the gradient can be modulated by varying the cell density of the TMCS and the height of the gap between the two glass slides. The mathematical model described in this paper provides a predictive method of planning TMCS experiments.

Address correspondence to Rakesh K. Jain, PhD, Edwin L. Steele Laboratory, Department of Radiation Oncology, Massachusetts General Hospital,100 Blossom St, Cox-7, Boston,Massachusetts 02114. Electronic mail: jain@steele.mgh.harvard.edu

Mathematical models for the prediction of oxygen profiles within three-dimensional spheroids have been developed extensively and microelectrode measurements used to measure oxygen profiles within spheroids.[1,7,8,20,21,26] One comprehensive model by Casciari *et al.*[7] modeled the growth of spheroids based on gradients of oxygen, glucose, lactate ion, carbon dioxide, bicarbonate ion, chlorine ion, and hydrogen ion within the spheroids. Oxygen and glucose consumption rates as well as glucose diffusivities and cell growth rates were measured in the EMT6/Ro mouse mammary sarcoma cell line, and the spheroid growth rates, viable rim thickness, and nutrient consumption rates were predicted from the model. In their model, steady-state was assumed so that only the time-independent differential equations were solved. In the realm of spheroids, the utility of these models has typically been their ability to predict spheroid growth rates and determine the factors that contribute to the growth of spheroids.

The TMCS can also be modeled using standard diffusion equations with a consumption term for the depletion of oxygen and nutrients by the cells in the system.[17,18] The model used in this paper was originally applied to the TMCS by Hlatky *et al.*[18] to predict the viable border width of cells within the system. The present model builds on the prior studies and advances them in two ways: 1) the mathematical model predicts the time course of the evolution of oxygen and glucose concentration profiles, and 2) the predicted oxygen concentration profiles are directly validated by measurement of oxygen concentrations within the TMCS.

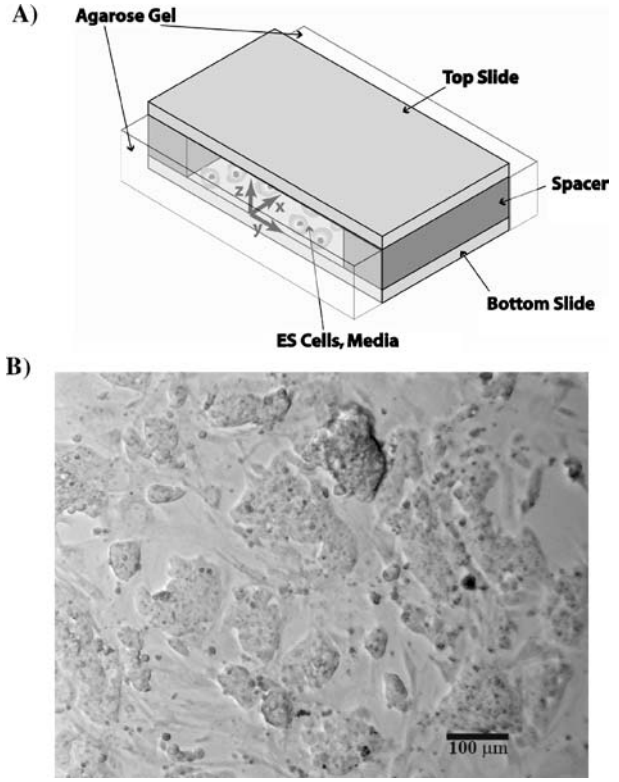

FIGURE 1. (A) Diagram of the Tissue-Mimetic Culture System (TMCS). The cells are "sandwiched" between two glass slides separated by a spacer of known height. Oxygen and nutrients from the media can only reach the central region of the system by diffusion, setting up oxygen gradients within the system as the cells consume oxygen. An agarose mold surrounds the system, which allows diffusion of small molecules such as oxygen and nutrients while preventing convective mixing of the fluid in contact with the cells. The x-direction is the direction of diffusion of oxygen and gradients, the y-direction is parallel to the edge of the system, and the z-direction is perpendicular to the surface on which the cells are grown. (B) Light microscopic image of ES cells growing within the TMCS at the time of the addition of the top slide to the system, demonstrating the morphology and growth pattern of the cells within the TMCS.

MATERIALS AND METHODS

Theoretical Model of Tissue-Mimetic Culture System

The TMCS is illustrated in Fig. 1(a). As oxygen and nutrients diffuse into the system from the edge of the culture ($x = 0$ mm), they are consumed by the cells which are seeded on the bottom slide. A steady-state is established when the diffusion into the system is balanced by cellular consumption within the system. The following assumptions are made:

1. Oxygen and glucose are the only components of interest within the model. It is well known that per-cell consumption of either oxygen or glucose depends on the concentration of both substances,[2] so both are accounted for within the model.
2. The cell number is assumed to be spatially and temporally constant over the 24-hour period of interest. In reality, the cells are dividing and growing during the time of interest, and likely at different rates in different locations due to the dependence of cell proliferation on oxygen concentration. Thus, the model is primarily valid at early time points before the cell density changes significantly.
3. The per-cell consumption rates of oxygen and glucose do not depend explicitly on time, only on the concentrations of oxygen and glucose at any given location.
4. The oxygen and glucose concentrations are assumed to be independent of location in the y-direction (see Fig. 1(a)), as measurements are made in the center of the slide (approximately 3 cm from the edge of the culture in the y-direction).
5. The oxygen and glucose concentrations are independent of z-direction (above the cells). The validity of this assumption will be assessed in the Discussion section.

6. The agarose gel does not limit the diffusion of glucose or oxygen into the TMCS. As seen in Fig. 1(a), diffusion through the agarose occurs in 3 dimensions, as glucose and oxygen can also diffuse in through the top of the agarose. The shortest diffusion distance through the agarose is approximately 0.5 mm, and the characteristic diffusion times of oxygen and glucose across this distance are 1.4 min and 4.6 min, respectively. It will be shown that the characteristic consumption times of oxygen and glucose within the TMCS for the experiments performed herein are approximately 11 min and 11 hours, respectively. Thus, it is assumed that the contribution of diffusion through the agarose gel can be disregarded in the solutions of the proposed mathematical model.
7. The ES cells form a monolayer within the TMCS. Figure 1(b) shows a light microscopic view of the ES cells within the system soon after the introduction of the top slide. While the cells tend to clump together, the clumps are spread thin so that the monolayer approximation is likely valid. Although the local cell density may vary from point to point, it is assumed that the macroscopic, average cell density will determine the overall oxygen consumption, and thus the oxygen gradient, within the TMCS.

For these assumptions, the diffusion equations reduce to two coupled, one-dimensional time-dependent partial differential equations:

$$\frac{\partial p_{\mathrm{O}}(\mathrm{x,t})}{\partial \mathrm{t}} = D_{\mathrm{O}}\frac{\partial^2 p_{\mathrm{O}}(\mathrm{x,t})}{\partial \mathrm{x}^2} - Q_{\mathrm{O}}(p_{\mathrm{O}}, C_{\mathrm{G}})\frac{N}{Z_G} \quad (1)$$

$$\frac{\partial C_{\mathrm{G}}(\mathrm{x,t})}{\partial \mathrm{t}} = D_{\mathrm{G}}\frac{\partial^2 C_{\mathrm{G}}(\mathrm{x,t})}{\partial \mathrm{x}^2} - Q_{\mathrm{G}}(p_{\mathrm{O}}, C_{\mathrm{G}})\frac{N}{Z_G} \quad (2)$$

where $p_{\mathrm{O}}(\mathrm{x,t})$ and $C_{\mathrm{G}}(\mathrm{x,t})$ are the location- and time-dependent partial pressure of oxygen and concentration of glucose, respectively; D_{O} and D_{G} are the diffusional constants of oxygen[13,24] and glucose[19] in water at 37°C ($D_{\mathrm{O}} = 3 \times 10^{-5}$ cm^2 sec^{-1}; $D_{\mathrm{G}} = 9 \times 10^{-6}$ cm^2 sec^{-1}); N is the number density of cells per unit surface area in the TMCS (cells cm^{-2}); Z_G is the gap height of the system; and $Q_{\mathrm{O}}(p_{\mathrm{O}},C_{\mathrm{G}})$ and $Q_{\mathrm{G}}(p_{\mathrm{O}},C_{\mathrm{G}})$ are the per-cell consumption rates of oxygen and glucose that are dependent on oxygen and glucose concentrations. The quantity N/Z_G is a valid measure of the volume density of cells within the TMCS as long as the assumption of z-independence of nutrient concentration holds.[17,18]

The initial and boundary conditions are set such that the initial concentrations of oxygen and glucose, as well as the concentration at either edge of the TMCS, are set at the bulk media concentrations ($p_{\mathrm{O}} = 160$ mmHg; $C_{\mathrm{G}} = 3.5$ mg ml^{-1}). The oxygen and glucose consumption rates were experimentally determined, including their dependence on glucose and oxygen concentrations. The combined parameter, N/Z_G, was taken to be an experimentally determined parameter that can be varied by changing either the cell density or the gap height in the system.

Six useful parameters can be calculated from the mathematical model: the diffusion time for oxygen and glucose to diffuse to the center of the TMCS ($T_{\mathrm{D,O}}$ and $T_{\mathrm{D,G}}$); the consumption time necessary for the total amount of oxygen or glucose at any location to be consumed ($T_{\mathrm{C,O}}$ and $T_{\mathrm{C,G}}$); and the penetration distance for oxygen and glucose (X_{O} and X_{G}), which is the characteristic diffusion distance for each substance during the time period $T_{\mathrm{C,O}}$ and $T_{\mathrm{C,G}}$, respectively. If W is the entire width of the glass slide (2.5 cm) and $p_{\mathrm{O,a}}$ and $C_{\mathrm{G,a}}$ are the ambient oxygen partial pressure and glucose concentration, then the listed parameters can be estimated as follows:

$$T_{\mathrm{D,O}} = \frac{(W/2)^2}{D_{\mathrm{O}}} = 14\,\mathrm{hr} \quad (3)$$

$$T_{\mathrm{D,G}} = \frac{(W/2)^2}{D_{\mathrm{G}}} = 48\,\mathrm{hr} \quad (4)$$

$$T_{\mathrm{C,O}} = \frac{p_{\mathrm{O,a}}}{Q_{\mathrm{O}}(N/Z_G)} \quad (5)$$

$$T_{\mathrm{C,G}} = \frac{C_{\mathrm{G,a}}}{Q_{\mathrm{G}}(N/Z_G)} \quad (6)$$

$$X_{\mathrm{O}} = (D_{\mathrm{O}}T_{\mathrm{C,O}})^{0.5} \quad (7)$$

$$X_{\mathrm{G}} = (D_{\mathrm{G}}T_{\mathrm{C,G}})^{0.5} \quad (8)$$

Cell Lines and Culture Conditions

Mouse embryonic stem (ES) cells that expressed (*HIF-1α*$^{+/+}$) or lacked (*HIF-1α*$^{-/-}$) hypoxia-inducible-factor (HIF)-1α, a transcription factor upregulated by low oxygen concentration, were generated as described previously.[6] Cells were maintained at low passage number in Dulbecco's Modified Eagle's Medium (Invitrogen-Gibco, Carlsbad, CA) with high glucose (4.5 mg ml^{-1}) and 20% heat-inactivated fetal calf serum, supplemented with non-essential amino acids (0.1 mmol l^{-1}), sodium pyruvate (1 mmol l^{-1}), L-glutamine (6 mmol l^{-1}), 2-mercaptoethanol (10 μmol l^{-1}), penicillin/streptomycin (100 units ml^{-1}, 100 μg ml^{-1}), and leukemia inhibitory factor (ESGro, Chemicon International, Temecula, CA, 1000 units ml^{-1}) to prevent differentiation. Cells were grown on an inactivated primary mouse embryonic fibroblast feeder layer (Specialty Media, Chemicon International, Temecula, CA) at a density of 50,000 fibroblasts cm^{-2}.

Tissue-Mimetic Culture System

The TMCS has been described previously.[15,17] Briefly, the ES cells (50% *HIF-1α*$^{+/+}$; 50% *HIF-1α*$^{-/-}$) were seeded on a glass microscope slide at a density of 100,000 cells cm^{-2}. The cells were grown for 24 h at 37°C in 5% CO_2 in air. A second microscope slide was then placed directly over the first slide, with a 350 μm gap between the two slides as a result of fixed-thickness spacers at either end of the glass slides (see Fig. 1(a)). A 2-mm thick agarose gel was formed around the system so that no convection occurred due to inadvertent movement of the culture dish. The cells in the transparent TMCS could be visualized microscopically. A temperature-controlled stage was utilized to maintain cells at 37°C during the measurement of oxygen concentrations over a 3 h time period at various locations in the system.

Glucose Consumption Rates

Glucose consumption rates of ES cells were measured in a manner similar to Hlatky *et al.*[18] Briefly, ES cells were seeded in 6-cm dishes on an inactivated fibroblast layer at a seeding density of 100,000 cells cm^{-2} and 500,000 cells cm^{-2}. Separate dishes were also seeded with fibroblasts alone to measure the contribution of the fibroblasts to glucose consumption. The cells were allowed to grow for 24 h in normal cell culture conditions. At that time, the cell culture media was changed to fresh media and half of the dishes were placed into a normoxic cell culture incubator, while the other half were placed in a hypoxic chamber supplied with an artificial environment of 1% oxygen and 5% carbon dioxide in nitrogen in a 37°C culture room. Every 6–10 h for the next 48 h, one fifth of the cell culture media was removed for glucose measurements and replaced with an equal amount of fresh media to replenish the glucose and nutrients consumed by the cells. In separate 24-well plates, the ES cells were seeded at the same cell densities and cultured under the same conditions. At each time point for which media was removed for glucose measurements, two wells of each condition were trypsinized and counted by hemocytometer. The media taken from the 6-cm dishes was analyzed for glucose concentration using a glucose assay kit (Sigma, St. Louis, MO), and the hemocytometer counts were used to measure cell density at each time point (cells cm^{-2}). The glucose consumed per area of the cell culture dish was plotted vs. time, and the slope of the curve at each time point was calculated to obtain the glucose consumption rate. The slope was divided by the total cell density at each measured time point to give the per-cell glucose consumption rate (Q_G).

Oxygen Consumption Rate: Stirred-Chamber Method

The oxygen consumption rate of *HIF-1α*$^{+/+}$ and *HIF-1α*$^{-/-}$ ES cells in normal culture media (3.5 mg ml^{-1} glucose) was measured in a fiber-optic oxygen monitoring system according to the manufacturer's instructions (Instech Laboratories, www.instech.com/manuals/). Briefly, cells were trypsinized and resuspended in fresh ES media. Cell concentration and viability were determined by fluorescence-based cell counting and membrane integrity tests using a flow cytometer (Guava PCA, Guava Technologies, Hayward, CA). The cells were concentrated to $5-6\times10^6$ cells ml^{-1}. Cells were suspended in fresh media and sealed in a 200 μl stirred titanium water-jacketed oxygen-impermeable chamber maintained at 37°C (Instech Laboratories, Plymouth Meeting, PA). The time-dependent partial pressure of oxygen (p_O) within the chamber was recorded with a fluorescence-based oxygen sensor (Ocean Optics, Dunedin, FL), and the decrease in oxygen tension vs. time curve was fit to a straight line. The oxygen tension was calibrated during each experiment both at room air concentrations ($p_O = 160$ mmHg) and after the oxygen has been fully consumed from the chamber ($p_O = 0$ mmHg). The maximal oxygen consumption rate (OCR) was evaluated by the equation $Q_O = (dp_O/dt) \times k_O/C$, where k_O is the solubility of oxygen in water at 37°C (1.19 nmol mmHg^{-1} ml^{-1}) and C is the concentration of cells in the suspension (cells ml^{-1}).

Oxygen Consumption Rate: Oxygen Biosensing Plate Method

In order to obtain high-throughput measurements of oxygen consumption rate at various glucose concentrations, an oxygen biosensing plate was used as described by Guarino *et al.*[14] The oxygen-sensing microplate used in these experiments was the BD Oxygen Biosensor (OBS) system (BD Biosciences, Bedford, MA). These plates incorporate an oxygen-sensitive ruthenium-based fluorophore in a silicone rubber matrix in the bottom of each well of a standard 96-well microplate.[29] The ES cells were seeded in quadruplicate at a density of 25,000 cells per well in five different glucose concentrations (3.5 mg ml^{-1}, 2.6 mg ml^{-1}, 1.6 mg ml^{-1}, 1.0 mg ml^{-1}, and 0 mg ml^{-1} glucose). HEPES buffer was added to the media at 25 mM. The microplates were incubated at 37°C in a temperature controlled microplate fluorometer (Fluroskan Ascent, Thermo Electron Corporation) for 24 h, and the fluorescence from the wells was measured every 4 h (excitation: 485 nm, emission: 620 nm). The fluorescence readings were converted to oxygen concentrations, and the oxygen consumption rates was estimated using the techniques described by Guarino *et al.*[14] The per-cell oxygen consumption rate was calculated by dividing the total oxygen consumption rate (extrapolated to time zero) by the initial number of cells in each well.

Phosphorescence Quenching Microscopy

Oxygen tension measurements were made *in vitro* using a phosphorescence quenching microscopic technique

described in Ref. 16. The oxygen-dependent porphyrin probe (OxyPhor R0; Harvard Apparatus, Holliston, MA)[25,28] was bound to albumin according to the manufacturer's instructions. The final albumin-bound porphyrin solution was diluted to 5 mg ml^{-1} and mixed 1:10 with ES media with HEPES buffer added (25 mM). The porphyrin-containing media was added to the TMCS shortly before the top slide of the culture system was put in place. The oxygen measurements were made at 1-mm intervals across the TMCS slide or a control slide by placing the culture system within a temperature controlled microscope stage designed to maintain the temperature at 37°C. The stage was placed on an automated stage, and the stage control was set to automatically move the stage in 1-mm increments from the edge of the TMCS to the center. The phosphorescence signal of the oxygen-dependent phosphor was detected at >630 nm with a photomultiplier tube after a 540-nm flashlamp excitation. The signal was averaged on a digital oscilloscope before computer storage. *In vitro* decay signals were fitted with an exponential function and the exponential decay time constants were converted to p_O values according to the Stern-Volmer equation:

$$1/\tau = 1/\tau_o + k_q(p_O) \tag{9}$$

where τ is the time constant of decay, τ_o is the time constant of decay in the absence of oxygen, and k_q is a quenching constant. The constants τ_0 and k_q in Eq. 9 were obtained by calibration of the system as described in Ref. 16.

Statistical Analysis

The mathematical model in Eqs. (1–2) requires 7 experimentally determined parameters (see Results): (1) the slope of the glucose consumption rate equation at low oxygen concentrations in Eq. 10; (2,3) the slope and intercept of the oxygen dependence of glucose consumption rate in Eq. 11; (4,5) the slope and intercept of the glucose dependence of the oxygen consumption rate in Eq. 13; (6) the kinetic parameter, K_M, describing the dependence of oxygen consumption rate on oxygen concentration in Eq. 12; and (7) the initial cell density, N/Z_G, in Eqs. (1–2). The uncertainty of model predictions resulting from measurement errors of these parameters was accounted for by the following procedure: First, the means and the variance-covariance matrix describing the statistical distribution of parameter estimates were determined from experimental data. Second, 1000 sets of parameters were drawn at random from a multivariate normal distribution using the same means and variance-covariance, and the mathematical model was solved for each set of parameters. Third, the 95% confidence intervals were determined from the 2.5-th and 97.5-th percentiles of the generated set of model predictions. The experimental measurements were compared graphically to model predictions including the 95% confidence interval. In addition, we calculated generalized R-squares[3] for the experimental data as a measure of goodness-of-fit to the theoretical predictions.

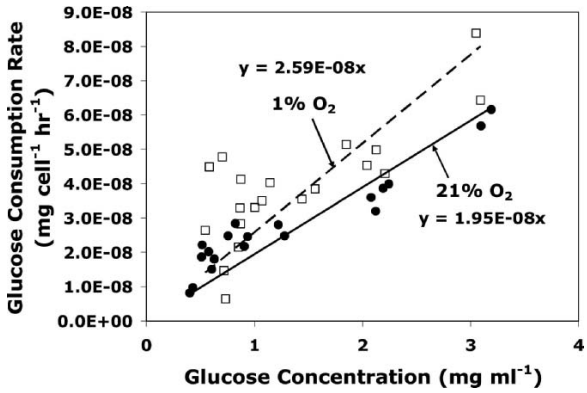

FIGURE 2. Glucose consumption rates for *HIF-1α*$^{+/+}$ and *HIF-1α*$^{-/-}$ cells (data combined) at various glucose concentrations in normoxia (21% O$_2$; closed circles) and hypoxia (1% O$_2$; open squares). The solid lines are linear least square fits of the data with the lines forced through the origin (no glucose consumption at zero glucose conditions). There was significant scatter of the data at conditions of combined low glucose and low oxygen concentrations.

Results

Glucose Consumption Rates

In Fig. 2, the glucose consumption rate of the ES cells is plotted against glucose concentration. The normoxic ($p_O = 160$ mmHg) and hypoxic ($p_O = 7.6$ mmHg) glucose consumption rates are plotted separately to obtain the oxygen dependence of the glucose consumption rate. It can be seen that glucose consumption rate is roughly linear with glucose concentration, indicating that for these cells, Michaelis-Menten saturation conditions have not been reached. The data for *HIF-1α*$^{+/+}$ and *HIF-1α*$^{-/-}$ ES cells, as well as data from experiments with different seeding densities, were combined, as these factors did not affect the relationship between glucose consumption rate and glucose concentration. Since glucose consumption rate should fall to zero at zero glucose concentration, linear approximations of the glucose dependence were forced to intercept the origin. This linear approximation fits the data reasonably well at higher glucose concentrations; however, the goodness of fit decreases as the glucose concentration falls below 1 mg ml^{-1}. As a first approximation, this linear fit was used for the glucose dependence of the glucose consumption rate in the analytic solution of Eqs. (1–2).

Tziampazis and Sambanis[27] measured glucose consumption rate as a function of oxygen concentration in mouse insulinoma βTC3 cells and found that glucose consumption rate was constant at the normoxic value down to an oxygen partial pressure (p_O) of approximately 13–15 mmHg. Below this value, the glucose consumption rate increased

linearly to a maximum value at anoxic conditions. This well-established rise in glucose consumption under hypoxia, the Pasteur effect, is observed for many cell lines.[2] Balin *et al.*[4] reported no significant difference in glucose consumption rate in WI-38 lung embryonic fibroblasts from 26–134 mmHg, and an increased glucose consumption rate when grown at a p_O of 7.8 mmHg. In a model of coupled glucose and oxygen consumption in V79 Chinese hamster lung cells, Hlatky *et al.*[18] also assumed an approximately linear rise in glucose consumption rate beginning at a p_O of approximately 30 mmHg and rising to a maximum value of twice the normoxic rate in anoxic conditions. The embryonic stem cells used in the TMCS experiments had a 33% higher glucose consumption rate at a p_O of 7.6 mmHg than at normoxic conditions (see Fig. 2), consistent with the above results reported in the literature. For the purposes of the solution of Eqs. (1–2), the glucose consumption rate is assumed constant from 15–160 mmHg at the value measured for 160 mmHg ($Q_{G,normoxic}$). Below 15 mmHg, the glucose consumption rate is assumed to rise linearly by the equation, Q_G[mg cell^{-1} hr^{-1}] = $(-0.045p_O$[mmHg] + 1.67)*$Q_{G,normoxic}$ [mg cell^{-1} hr^{-1}], based on the glucose consumption rates experimentally measured at 21% and 1% oxygen.

The final expressions used for the glucose consumption rate in the solution of Eqs. (1–2) are:

If $p_O \geq 15$ mmHg:

$$Q_G = 1.95 \times 10^{-8} \times C_G \quad (10)$$

If $p_O < 15$ mmHg:

$$Q_G = (-0.045 p_O + 1.67) \times 1.95 \times 10^{-8} \times C_G \quad (11)$$

where Q_G is in mg cell^{-1} hr^{-1}, p_O is in mmHg, and C_G is in mg ml^{-1}.

Oxygen Consumption Rates

The oxygen consumption rates measured with the stirred chamber method for *HIF-1α*$^{+/+}$ and *HIF-1α*$^{-/-}$ ES cells at a glucose concentration of 3.5 mg ml^{-1} are shown in Fig. 3(a). The oxygen consumption rate of the *HIF-1α*$^{-/-}$ cells was approximately 15% higher ($p = 0.02$) than that of the *HIF-1α*$^{+/+}$ cells. For the purpose of the solution of the mathematical model, the average value of the oxygen consumption rate (OCR) for both cell types, 13.7×10^{-5} nmol cells^{-1} hr^{-1}, was used. This assumption should introduce minimal error because 1) the difference in OCR between the two cell types is small, and 2) the experiments are performed with a mixture of 50% *HIF-1α*$^{+/+}$ cells and 50% *HIF-1α*$^{-/-}$ cells. Thus, the actual consumption rate experienced within the TMCS should be close to the average value between the two cell types.

The oxygen consumption rate of cells generally follows Michaelis-Menten kinetics with respect to oxygen

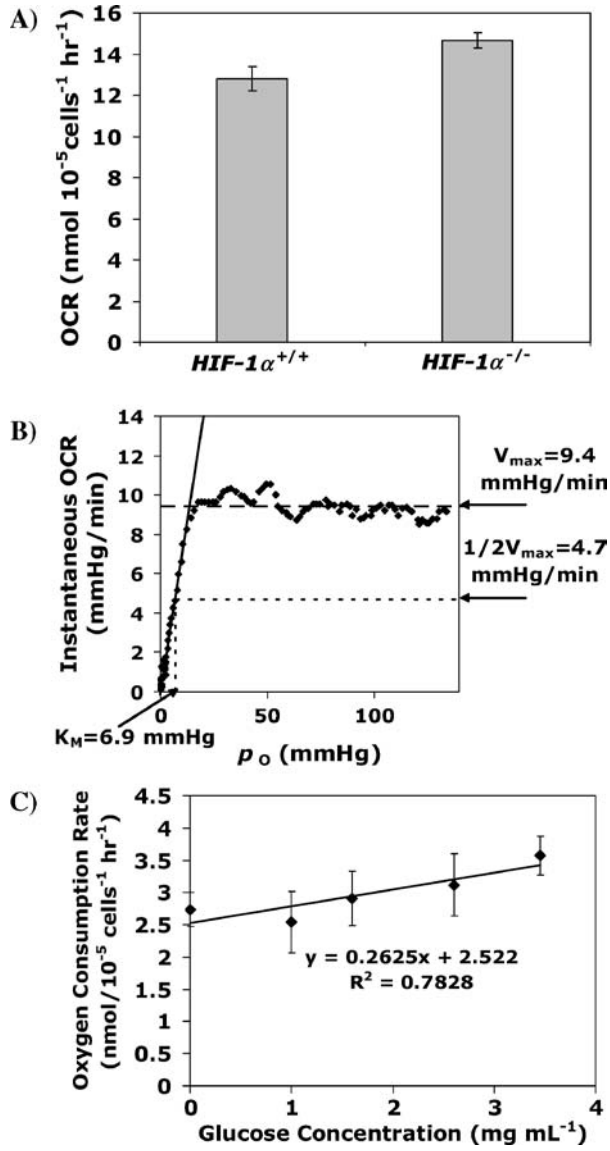

FIGURE 3. Oxygen consumption rate of ES cells. (A) Stirred-chamber measurements: Average values of 6 replicates for each cell type. The *HIF-1α*$^{-/-}$ cell OCR is significantly higher than that of the *HIF-1α*$^{+/+}$ cells ($p = 0.02$). The error bars indicate the standard error of the mean for the measurements. (B) Method of calculation of K_M for oxygen dependence of OCR. The data is a representative curve from one of the stirred-chamber measurements of OCR. The glucose concentration used in this experiment was 3.5 mg/ml. The solid line is a best fit line through the initial rising points of the curve, and the small dashed lines demonstrate the method used to calculate K_M: the p_O value at which the solid line crosses one half of the V_{max} value. (C) Biosensor plate measurements: Combined data of oxygen consumption rates measured at various glucose concentrations for *HIF-1α*$^{+/+}$ and *HIF-1α*$^{-/-}$ ES cells. Average values of 5–7 replicates for each data point. The error bars indicate the standard error of the mean for the measurements. As described in the text, these experiments were begun at ambient oxygen concentrations ($p_O = 160$ mmHg), and the change in oxygen concentration over time was measured using the biosensor plate technique. This technique underestimated the absolute oxygen consumption rate by a factor of 4 compared to the stirred chamber method.

concentration:[5,10,18,30]

$$Q_O = \frac{V_{max} p_O}{K_M + p_O} \tag{12}$$

where V_{max} is the maximum consumption rate (at normoxic conditions) and K_M is the half-maximal oxygen concentration at which the oxygen consumption rate is half of its maximum rate. K_M values typically fall in the range of 0.5–10 mmHg.[5,10,18,30] The OCR data obtained from the stirred chamber measurements was used to estimate the K_M value for ES cells (Fig. 3(b)). The instantaneous slope of the stirred-chamber curve was plotted against the oxygen tension for each OCR measurement, and a straight line was fit through the initial rising portion of the resulting curve. The point at which this line crossed the value corresponding to one half of the maximal OCR was taken as the K_M for that curve. The average value of 12 measurements by this method gave a K_M for the ES cells of 5.2 ± 0.9 mmHg (mean $\pm$ SEM).

The glucose dependence of oxygen consumption rate as measured by the oxygen biosensor (OBS) plate method is shown in Fig. 3(c). This 96-well plate method has been described by Guarino *et al.*[14] and has the advantage of allowing multiple measurements in parallel. While this method has been shown to be very accurate at measuring relative oxygen consumption rates within an experiment, the absolute values of oxygen consumption rate (OCR) measured by the OBS method underestimated the OCR by a factor of 4.0, as determined by the more accurate stirred-chamber method (compare Fig. 3(a) to Fig. 3(c)). Therefore, the plate method was used to calculate relative values of OCR at various glucose concentrations, and then the predicted values were scaled appropriately by a factor of 4.0. The OCR drops slightly with decreasing glucose concentration, as shown in Fig. 3(c). The final expression for oxygen consumption accounts for this glucose dependence, the Michaelis-Menten dependence on oxygen concentration, and the scaling factor obtained from comparing the OBS method with the stirred-chamber method:

$$Q_O(\text{nmol } 10^{-5} \text{ cells}^{-1} \text{ hr}^{-1}) = (1.05\, C_G + 10.08) \times \frac{p_O}{p_O + 5.2} \tag{13}$$

where C_G is in mg ml^{-1} and p_O is in mmHg.

Predictions of Mathematical Model

The theoretical predictions of the glucose and oxygen profiles in the TMCS are shown in Fig. 4 for 3 different seeding densities. In the solution of the differential equations, the quantity N/Z_G is taken to be a single adjustable parameter, corresponding to an effective volume cell density of cells within the system. Variation of the parameter N/Z_G changes two fundamental parameters of the system, the time for the concentration profiles to reach steady-state, and the penetration depth of each nutrient, defined as the distance over which the gradient occurs at steady-state. As long as the consumption time, T_C, is less than the diffusion time, T_D (14 hr for oxygen, 48 hr for glucose), for the system, then the time to steady-state can be approximated by the consumption times, $T_{C,O}$ and $T_{C,G}$, for oxygen and glucose, respectively. Likewise, the penetration depths are approximated by the diffusion distances, X_O and X_G, calculated from Eqs. (7–8). The variation of these parameters as a function of the adjustable parameter, N/Z_G, is shown in Fig. 5(a) and 5(b).

Experimental Validation of Model

A TMCS experiment as described in Materials and Methods was performed to measure the developing oxygen profiles to compare the experimental measurements with the predictions of the model. The oxygen tension measurements are shown in Fig. 6(a) (data points) for various time points up to 3 h after starting the experiment. The initial measurements were taken before the top slide was added to the culture. The phosphorescence quenching technique as performed is only accurate from 0–60 mmHg. Above this range, the measured phosphorescence decay half-life becomes constant due to limitations of the optical system and is no longer inversely related to oxygen tension. Therefore, the measurements above 60 mmHg in Fig. 6 correspond to some value between 60 mmHg and 160 mmHg (room air). Figure 6(a) indicates that a steady-state profile was reached experimentally within 20 min and remained fairly stable for at least 3 h, with a penetration distance of approximately 2 mm.

The cell densities 24 h after seeding with 100,000 cells cm^{-2} correspond to $(3.2 \pm 0.3) \times 10^5$ cells cm^{-2} (data taken from cell counts made for glucose consumption rate measurements), which corresponds to an N/Z_G of 9.1×10^6 cells cm^{-3}. For this cell density, the theoretical model predicts that the steady-state oxygen profile will develop in approximately 11 min, and the solid line in Fig. 6(a) shows the predicted steady-state profile. The dashed lines in Fig. 6(a) show the 95% confidence interval accounting for statistical variation in data used to estimate the parameters in the mathematical model. It can be seen that the experimental data after steady-state is reached mostly agrees with the expected range of solutions predicted from the theoretical model. The generalized R-squares measuring goodness-of-fit of the model predictions to oxygen tension measurements at 1–12 mm from the sandwich edge were 0.986 at 20 min, 0.828 at 2 h, and 0.994 at 3 h.

While the theoretical model only predicts the profiles for a constant cell density, the effects of proliferation on the steady-state oxygen profile were estimated by solving the model with a cell density corresponding to 24 h of proliferation within the TMCS. This cell density was estimated from the cell counting experiments performed during the

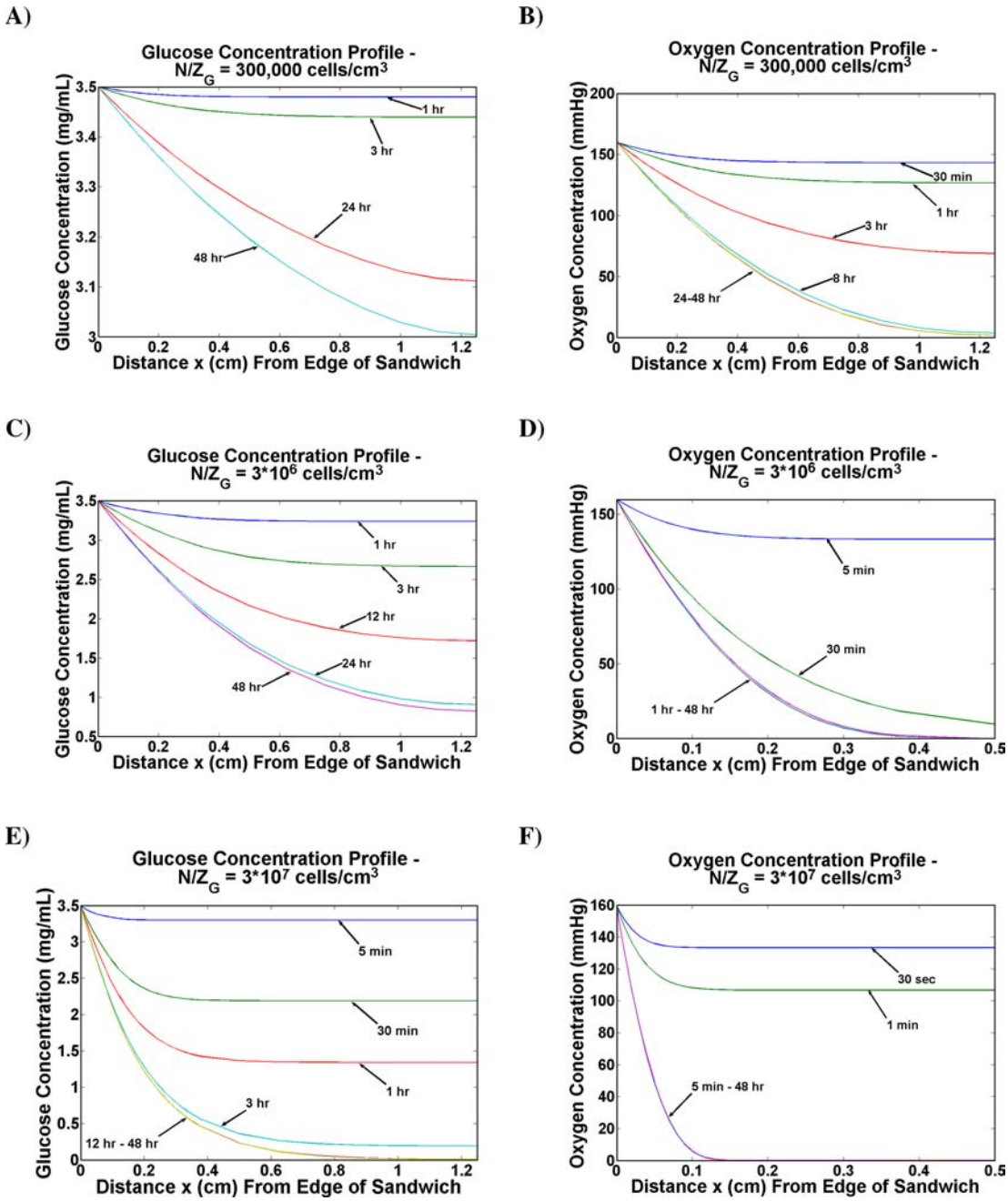

FIGURE 4. Glucose (A,C,E) and oxygen (B,D,F) profiles from the edge of the TMCS for seeding densities of (A,B) 3×10^5 cells cm^{-3}, (C,D) 3×10^6 cells cm^{-3}, and (E,F) 3×10^7 cells cm^{-3}. The separate curves are labeled with the corresponding time points, demonstrating the development of the steady-state profiles over time. Note: In C-F, the length scale for the oxygen profile differs from the length scale for the glucose profile to focus on the oxygen gradient, which occurs within the first 5 mm from the edge.

measurement of glucose consumption rate (see Materials and Methods). An average of the proliferation rate of normoxic and hypoxic cells was used to gain a rough estimate of the cell density within the system. The average cell density obtained in this way was $(7.6 \pm 0.5) \times 10^5$ cells cm^{-2}, giving an N/Z_G of 2.2×10^7 cells cm^{-3}. The dashed line in Fig. 6(b) is the predicted steady-state oxygen profile for the TMCS at this higher cell density.

DISCUSSION

In this paper, a mathematical model was used to predict the initial oxygen and glucose concentration profiles within the TMCS, an ideal system for studying the effects of the microenvironment on cells in culture. The glucose consumption rates and oxygen consumption rates were measured for mouse embryonic stem cells, and empirical

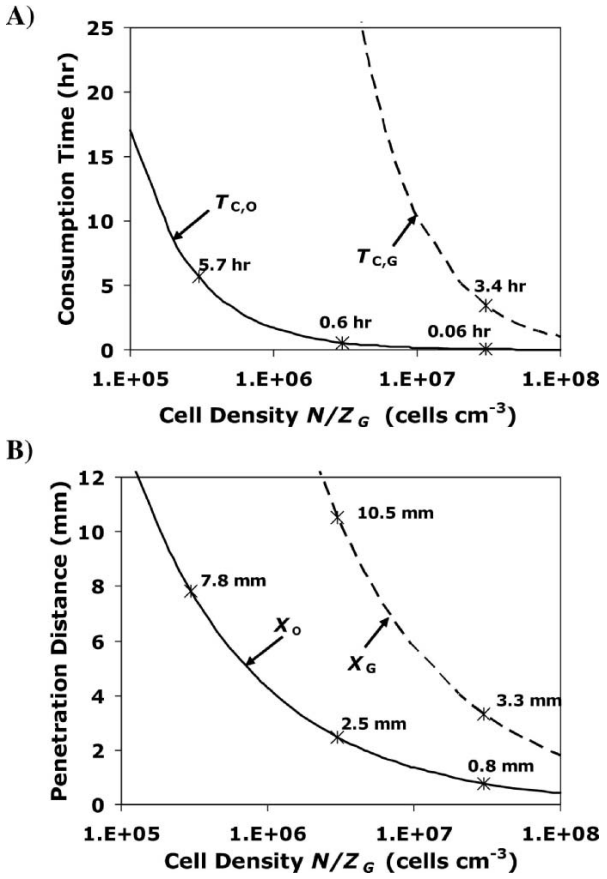

FIGURE 5. (A) Characteristic times for consumption of all oxygen or glucose at a given location within the TMCS as a function of cell density. The data labels (crosses) mark the values for the cell densities used to generate Fig. 4. This gives an estimate of the time for the system to reach steady-state. (B) Characteristic penetration distances for oxygen or glucose within the TMCS as a function of cell density. The data labels (crosses) mark the values for the cell densities used to generate Fig. 4. This gives an estimate of the distance over which the oxygen and glucose gradients span within the system.

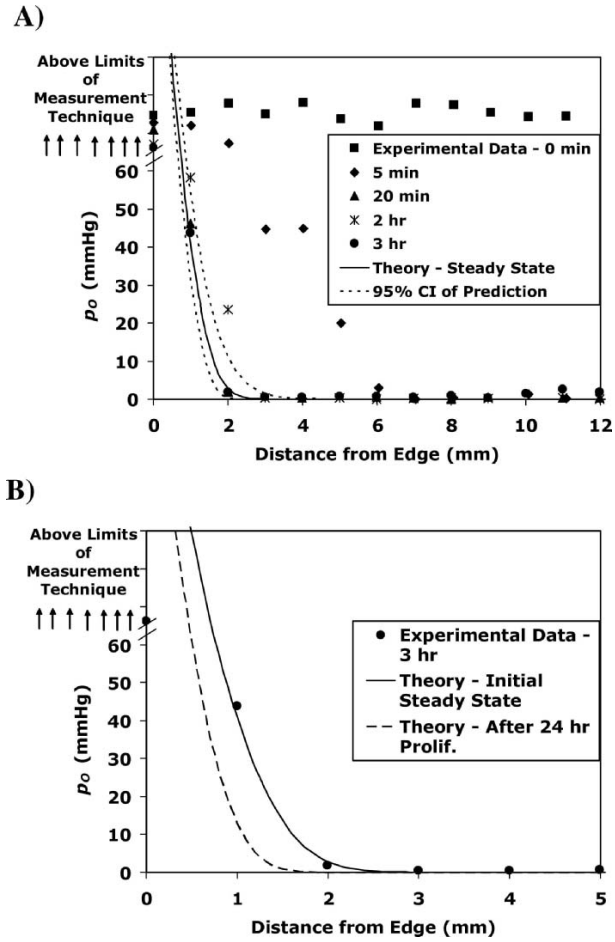

FIGURE 6. (A) The data points show experimental measurements of p_O within the TMCS started 24 h after seeding at a density of 100,000 cells cm^{-2}. The cell density at this time corresponds to $N/Z_G = 9.1 \times 10^6$ cells cm^{-3}. The oxygen profile reached steady-state within 20 min. The theoretical model predicts that the oxygen profile will reach steady-state in 11 min (Fig. 5(a)), depicted by the solid line. The dashed lines give the 95% confidence interval of the model prediction based on 1000 simulations using normally distributed randomly generated model parameters. ■, Experimental measurements at the beginning of the experiment; ♦, Experimental measurements 5 min after the addition of the top slide to the TMCS; ▲, Experimental measurements 20 min after the addition of the top slide to the TMCS; *, Experimental measurements 2 h after the addition of the top slide to the TMCS; ▲, Experimental measurements 3 h after the addition of the top slide to the TMCS. (B) Comparison of predicted curves initially and after 24 h of proliferation. ▲, Experimental measurements 3 h after the addition of the top slide to the TMCS. The solid line gives the theoretical steady-state profile at $N/Z_G = 9.1 \times 10^6$ cells cm^{-3}. The dashed line gives the steady-state profile for a density of $N/Z_G = 2.2 \times 10^7$ cells cm^{-3}, corresponding to the density after 24 h of proliferation within the TMCS.

expressions for the glucose and oxygen dependence of the two consumption rates were developed. These expressions were used in the mathematical model to obtain explicit oxygen and glucose concentration profiles within the system. The only experimental parameter to be determined in the resulting model is the volume cell density of cells, which can be experimentally varied by changing either the seeding cell density within the TMCS or the gap height between the top and bottom slides. The oxygen profiles in the TMCS were experimentally measured in an ES cell system to validate the predictions of the model. *HIF-1α*$^{+/+}$ and *HIF-1α*$^{-/-}$ ES cells were used in preparation for future studies on the effects of HIF-1α on the behavior of ES cells within oxygen gradients. The experimentally determined oxygen profiles up to three hours after initiation of the TMCS at a cell density of 9.1×10^6 cells cm^{-3} were consistent with the theoretical predictions of the mathematical model. Unfortunately, there is no adequate quantitative, optical technique for measuring glucose concentrations non-invasively within the TMCS, so that the glucose concentration profiles could not also be validated experimentally.

The current model should be compared with previous modeling descriptions of both tumor spheroids and the

TMCS. Casciari *et al.*[7] in their model of the tumor spheroid, additionally account for the effects of pH, carbon dioxide, and other metabolic products and ions on the behavior of the cells within the spheroid. It would be useful in future development of the current models to determine the effect that these factors would have on the predicted oxygen and glucose concentration profiles. Particularly, the effect of pH on the consumption of glucose and oxygen should be evaluated. In the previous study,[7] a pH-dependent increase in oxygen consumption rate was seen as glucose concentration decreased. This change was not observed in the current study, but could potentially become important as the pH within the system changes over time. In another study,[8] both glucose consumption rate and oxygen consumption rate were found to depend on pH. While the current model did not account for pH effects, it still gave accurate predictions of the initial profile development within the TMCS. The ability of the model to accurately predict long-term profiles within the TMCS may be enhanced in future modifications by incorporating a model of pH effects on nutrient consumption rates, similar to Casciari *et al.*[7]

In a previous TMCS modeling study,[18] temporal changes in cell density were also incorporated into the mathematical model using measurements of cell density taken directly from the TMCS as inputs to the model. However, the goal of the current study was to develop a predictive model that could be used to design the experiments in advance, precluding the use of measurements from the system as inputs. Also, the primary focus of the current model was on describing the time course of the initial development of the concentration profiles, thus allowing an assumption of constant cell density. Obviously, some of the later time predictions in Fig. 4(a)–(f) would be affected by changes in cell density over time, as indicated after accounting for proliferation in Fig. 6(b). To incorporate the effects of cell proliferation on the model predictions directly, it will be necessary in future studies to measure cell proliferation rates as a function of both oxygen and glucose concentrations. Then, the cell density term, N, could be made dependent on oxygen and glucose concentration, while maintaining the predictive nature of the model for designing TMCS experiments.

The predictions of the mathematical model described herein required only a specification of the "volume" cell density, N/Z_G, to obtain estimates of the concentration profiles. In reality, the area cell density, N (cells cm^{-2}), and the gap height, Z_G, can be varied independently. The key limitation for changing the gap height is the desire to maintain constant oxygen and glucose concentrations in the gap above a particular location within the TMCS. The dimensionless Damköhler number is a ratio of the characteristic diffusion time for oxygen or glucose to diffuse across the gap to the consumption time T_C for oxygen or glucose.[9] Therefore, the Damköhler number (Da) can be given for oxygen and glucose by the following expressions:

$$Da_O = \frac{\left(Z_G{}^2/D_O\right)}{p_{O,a}/(Q_O N/Z_G)} \tag{14}$$

$$Da_G = \frac{\left(Z_G{}^2/D_G\right)}{C_{G,a}/(Q_G N/Z_G)} \tag{15}$$

For the assumption of z-independence to hold, the diffusion time should be much less than the reaction time, corresponding to $Da<<1$. For the experimental conditions used in Fig. 6, the relevant Damköhler numbers are $Da_O = 0.07$ and $Da_G = 0.007$ for the initial cell density, and $Da_O = 0.2$ and $Da_G = 0.02$ for the cell density after 24 h of proliferation. Therefore, the assumption of z-independence is relatively good. Improvements in the Damköhler number could be obtained for a given N/Z_G by decreasing the gap height while decreasing the seeding density of cells by a proportional amount.

The TMCS experimental design can be useful in a wide variety of biological studies, and the theoretical model described herein is a valuable tool in the design of these TMCS experiments. Depending on the goal of the experiments, the predictions shown in Fig. 5 can be used to achieve desirable concentration profiles. For example, one area that would benefit from the use of this model system is the development and testing of pharmaceuticals. Pharmaceutical development typically relies on high-throughput testing of many comparison drugs to choose variations that have the greatest effect on cells in culture. However, when the drug encounters its target *in vivo*, there may be a wide variation in the microenvironment which it experiences that is not accounted for in these types of experiments. For example, in tumor chemotherapy, the chaotic and poorly perfused tumor vasculature leads to heterogeneous oxygen levels within the tumor.[16] If one wishes to study the effect of oxygen gradients on the response of cells to chemotherapies without a substantial change in glucose concentration, a TMCS experiment can be designed such that the oxygen gradient develops rapidly while the glucose concentration gradient develops over a much longer time. From Fig. 4(a) and (b), it is evident that appropriate conditions can lead to the development of oxygen gradients without an appreciable change in glucose concentrations.

Another important area of research that could benefit from the use of the TMCS and the models describing the microenvironmental changes within the system is the area of stem cell biology. The possibility of using stem cells in regenerative medicine requires the removal of the stem cells from their natural environment and placing them into a foreign environment. It is necessary to understand how the stem cells interact with their microenvironment.[11] For example, the potential of stem cells to be used in ischemic myocardium to regenerate the dead or dying heart muscle depends on the response of the stem cells to the ischemic

microenvironment, including the effects of hypoxia and HIF expression on stem cell behavior.[12] The ability of neural stem cells in the subventricular zone to replace neural cells damaged by brain injuries also depends on their protection against the effects of ischemia and hypoxia.[23] Also, the understanding of how hypoxia and HIF expression affects embryonic development and stem cell differentiation is important in understanding how hypoxic responses contribute to serious disease and developmental abnormalities.[22] The ability to accurately predict and control key microenvironmental conditions within the TMCS using models such as those described in this paper make this system ideal for furthering our understanding of stem cell biology and the therapeutic potential of stem cell techniques.

Several key limitations of the current model may become prohibitive for accurate stem cell studies without further developments both in the model and in our understanding of stem cell biology. It was previously noted that the assumption of a monolayer within the TMCS leads to the prediction of the average macroscopic gradients of oxygen and glucose, which does not account for local microgradients at the microscopic level. While this assumption did not affect the accuracy of the model predictions within the current system, further studies with more complex systems in which cells grow in multilayers with greater space in between islands of cells may require the incorporation of local gradients into the model. Also, if studies on stem cells are to be taken beyond the initial profile development, the effect of a heterogeneous population of differentiating cells must also be incorporated. In future developments of the model, it may be possible to account for varying cell proliferation rates, oxygen consumption rates, and glucose consumption rates within a mixed cell population. These modifications will require simultaneous progress in the understanding of stem cell proliferation and differentiation, as well as new assays for tracking the cell fates of a large population of stem cells. Ideally, future development of the TMCS model will parallel advances in the development of assays for the more careful study of stem cell biology and cell fate.

To summarize, this is the first report of the application of a time-dependent mathematical model to the TMCS to describe the development over time of the oxygen and glucose concentration profiles. The current work also provides predictive models for the design of TMCS experiments in which all of the parameters of the model were empirically determined rather than fit to experimental measurements. In addition, the current work provides the first validation within the TMCS of the oxygen profile predictions by direct, noninvasive measurement of oxygen concentrations. The TMCS and the models described herein provide a valuable system for the future studies of the effects of microenvironment on biological systems, including cancer models, response to pharmaceuticals, and the fast-growing field of stem cell biology.

ACKNOWLEDGMENTS

The authors thank the NIH for grant support (NIH grant P01 CA80124), and DMC thanks the Whitaker Foundation for fellowship support for this work. The authors would like to acknowledge William M. Deen (Chemical Engineering, MIT) for his scientific advice on the mathematical model used, Clark Colton and Daryl Powers (Chemical Engineering, MIT) for their assistance in measuring the stirred-chamber oxygen consumption rates, and Tim Padera and Ryan Lanning (Massachusetts General Hospital) for their editorial and scientific advice in the preparation of the manuscript.

REFERENCES

[1] Acker, H., G. Holtermann, J. Carlsson, and T. Nederman. Methodological aspects of microelectrode measurements in cellular spheroids. *Adv. Exp. Med. Biol.* 159:445–462, 1983.

[2] Aisenberg, A. C. *The Glycolysis and Respiration of Tumors*. New York: Academic Press, 1961.

[3] Anderson-Sprecher, R. Model comparisons and R^2. *Am. Statistician* 48:113–117, 1994.

[4] Balin, A. K., B. P. Goodman, H. Rasmussen, and V. J. Cristofalo. The effect of oxygen tension on the growth and metabolism of WI-38 cells. *J. Cell Physiol.* 89:235–249, 1976.

[5] Balis, U. J., K. Behnia, B. Dwarakanath, S. N. Bhatia, S. J. Sullivan, M. L. Yarmush, and M. Toner. Oxygen consumption characteristics of porcine hepatocytes. *Metab. Eng.* 1:49–62, 1999.

[6] Carmeliet, P., Y. Dor, J. M. Herbert, D. Fukumura, K. Brusselmans, M. Dewerchin, M. Neeman, F. Bono, R. Abramovitch, P. Maxwell, C. J. Koch, P. Ratcliffe, L. Moons, R. K. Jain, D. Collen, E. Keshert, and E. Keshet. Role of HIF-1alpha in hypoxia-mediated apoptosis, cell proliferation and tumour angiogenesis. *Nature* 394:485–490, 1998.

[7] Casciari, J. J., S. V. Sotirchos, and R. M. Sutherland. Mathematical modelling of microenvironment and growth in EMT6/Ro multicellular tumour spheroids. *Cell Prolif.* 25:1–22, 1992.

[8] Casciari, J. J., S. V. Sotirchos, and R. M. Sutherland. Variations in tumor cell growth rates and metabolism with oxygen concentration, glucose concentration, and extracellular pH. *J. Cell Physiol.* 151:386–394, 1992.

[9] Deen, W. M. *Analysis of Transport Phenomena*. New York: Oxford University Press, 1998.

[10] Foy, B. D., A. Rotem, M. Toner, R. G. Tompkins, and M. L. Yarmush. A device to measure the oxygen uptake rate of attached cells: Importance in bioartificial organ design. *Cell Transplant* 3:515–527, 1994.

[11] Fuchs, E., T. Tumbar, and G. Guasch. Socializing with the neighbors: Stem cells and their niche. *Cell* 116:769–778, 2004.

[12] Geng, Y. J. Molecular mechanisms for cardiovascular stem cell apoptosis and growth in the hearts with atherosclerotic coronary disease and ischemic heart failure. *Ann. N. Y. Acad Sci.* 1010:687–697, 2003.

[13] Grossmann, U., J. Carlsson, and H. Acker. Mathematical analysis of the influence of different supply conditions on pO_2 fields inside cellular spheroids by aid of finite element method. In: *Oxygen Transport to Tissue*, edited by H. I. Bicher and D. F. Bruley. New York: Plenum Press, 1983, pp. 481–486.

[14] Guarino, R. D., L. E. Dike, T. A. Haq, J. A. Rowley, J. B. Pitner, and M. R. Timmins. Method for determining oxygen

consumption rates of static cultures from microplate measurements of pericellular dissolved oxygen concentration. *Biotechnol. Bioeng.* 86:775–787, 2004.

[15]Helmlinger, G., M. Endo, N. Ferrara, L. Hlatky, and R. K. Jain. Formation of endothelial cell networks. *Nature* 405:139–141, 2000.

[16]Helmlinger, G., F. Yuan, M. Dellian, and R. K. Jain. Interstitial pH and pO_2 gradients in solid tumors *in vivo*: High-resolution measurements reveal a lack of correlation. *Nat. Med.* 3:177–182, 1997.

[17]Hlatky, L., and E. L. Alpen. Two-dimensional diffusion limited system for cell growth. *Cell Tissue Kinet.* 18:597–611, 1985.

[18]Hlatky, L., R. K. Sachs, and E. L. Alpen. Joint oxygen-glucose deprivation as the cause of necrosis in a tumor analog. *J. Cell Physiol.* 134:167–178, 1988.

[19]Li, C. K. The glucose distribution in 9L rat brain multicell tumor spheroids and its effect on cell necrosis. *Cancer* 50:2066–2073, 1982.

[20]Marusic, M., Z. Bajzer, J. P. Freyer, and S. Vuk-Pavlovic. Analysis of growth of multicellular tumour spheroids by mathematical models. *Cell Prolif.* 27:73–94, 1994.

[21]Mueller-Klieser, W., J. P. Freyer, and R. M. Sutherland. Influence of glucose and oxygen supply conditions on the oxygenation of multicellular spheroids. *Br. J. Cancer* 53:345–353, 1986.

[22]Ramirez-Bergeron, D. L., and M. C. Simon. Hypoxia-inducible factor and the development of stem cells of the cardiovascular system. *Stem Cells* 19:279–286, 2001.

[23]Romanko, M. J., R. Rola, J. R. Fike, F. G. Szele, M. L. Dizon, R. J. Felling, C. Y. Brazel, and S. W. Levison. Roles of the mammalian subventricular zone in cell replacement after brain injury. *Prog. Neurobiol.* 74:77–99, 2004.

[24]Thews, G., and H. Hutten. Biophysics of respiratory gas transport. In: *Biophysics*, edited by W. Hoppe, H. Lohmann, and H. Ziegler. Berlin: Springer-Verlag, 1983, 12.16: 503–514.

[25]Torres Filho, I. P., and M. Intaglietta. Microvessel pO_2 measurements by phosphorescence decay method. *Am. J. Physiol.* 265:H1434–1438, 1993.

[26]Tziampazis, E., and A. Sambanis. Modeling of cell culture processes. *Cytotechnology* 14:191–204, 1994.

[27]Tziampazis, E., and A. Sambanis. Tissue engineering of a bioartificial pancreas: Modeling the cell environment and device function. *Biotechnol. Prog.* 11:115–126, 1995.

[28]Vanderkooi, J. M., G. Maniara, T. J. Green, and D. F. Wilson. An optical method for measurement of dioxygen concentration based upon quenching of phosphorescence. *J. Biol. Chem.* 262:5476–5482, 1987.

[29]Wodnicka, M., R. D. Guarino, J. J. Hemperly, M. R. Timmins, D. Stitt, and J. B. Pitner. Novel fluorescent technology platform for high throughput cytotoxicity and proliferation assays. *J. Biomol. Screen* 5:141–152, 2000.

[30]Yarmush, M. L., M. Toner, J. C. Dunn, A. Rotem, A. Hubel, and R. G. Tompkins. Hepatic tissue engineering. Development of critical technologies. *Ann. N. Y. Acad Sci.* 665:238–252, 1992.